Conference Paper, Published Version

Talmon, A. M.; Wiesemann, Jens-Uwe

Influence of Grain Size on the Direction of Bed- Load Transport on Transverse Sloping Beds

Influence of Grain Size on the Direction of Bed-Load Transport on Transverse Sloping Beds

A.M. TALMON [*], J.-U. WIESEMANN [**]
[*] Delft Hydraulics, P.O. BOX 177, 2600 MH Delft, the Netherlands
[**] Institute of Hydraulic and Water Resources Engineering, Darmstadt University of Technology
Rundeturmstraße 1, 64283 Darmstadt, Germany

There is an intimate link between sediment transport and 3D-scour. In particular the role of transverse bed slope on the direction of sediment transport is determining 3D bed topographies. Hydraulic conditions, particle diameter and scale of the flow are important to the transverse slope effect. The present analysis focuses on the mechanical balance of particles travelling over ripples and dunes (grain size range: 0.09 to 0.9 mm). Fluid shear stresses on the grains, the average travelling height of particles in the turbulent boundary layer and drag coefficients of particles are considered. It is concluded that the transverse slope effect for fine grains is subject to viscosity, while for coarse grains it is not. It is shown how grain size is to be accounted for in the mathematical formula for transverse bed slope.

I. INTRODUCTION

The direction of bed-load transport over transverse sloping bed plays an important role in the calculation of the morphology of rivers, Struiksma et al. 1985. On a sloping bed, bed-load transport experiences a gravity component parallel with the bed surface, van Bendegom 1947. This is brought about by mechanical contact with the bed surface.

If this transverse bed slope effect is modelled too strong the calculated bed topographies will be flattened. If modelled too weak an unrealistic steep variation of bed topography will result. So calculated depths of 3D-scour holes, channel systems and hypsometry of estuaries will turn out to be wrong. Recent Delft3D calculations for Westerscheldt revealed such difficulties. It should be realized that a factor two difference in transverse slope coefficient will double the amplitude of calculated bed-topography variations.

World wide, the number of true data-points for transverse slope effect is worrying small (about 15, until Univ. Darmstadt commenced testing three years ago). Only dedicated well executed bed levelling experiments in straight flumes, see Figure 1, classify as true data points. Under such conditions one can focus on sediment transport processes without complications by 3D flow effects (secondary flow).

The force balance of transport in longitudinal and transverse direction specifies the actual sediment transport direction.

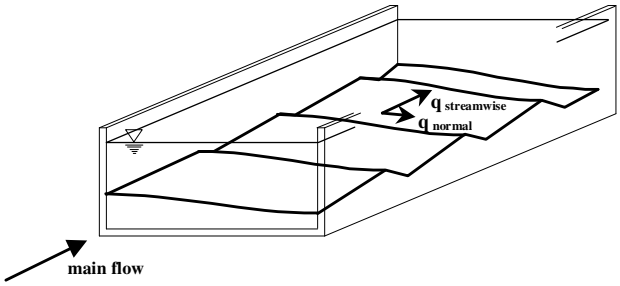

Figure I-1: Sand bed in bed-levelling experiment. For prolonged flow the bed levels horizontally.

The forces affecting a grain on a transverse bed slope are depicted in Figure I-2. In addition to the fluid drag force, the gravity force and the inclined bed turn the resulting force in downslope direction.

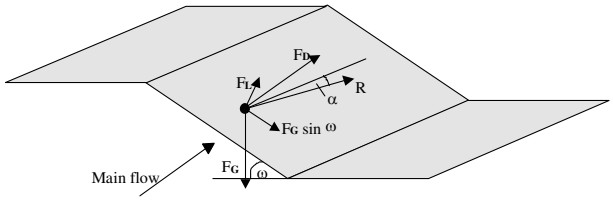

Figure I-2: Forces acting on grain on a transverse sloping bed: F_G=gravity, F_D=fluid drag, F_L=fluid lift, R=resulting force (transport direction), ω=angle transverse inclination.

In this paper it is shown that measured longitudinal and transverse bed-load transport in the laboratory, on different scales and different regimes, can be unified (fine and coarse sand). Account is given to grain stresses, the vectored force balance of particles on sloping beds, the transport velocity of bed-load and variation of drag coefficients. Discrepancies regarding the influence of grain diameter on the transverse slope effect, reported on in Talmon et al. 1995, are thus solved.

Unrightfully, the transverse slope effect has become a tuning parameter in the art of conducting numerical computations. This bad habit has to be eradicated as quickly as possible. Developers and users of mathematical models are provided an alternative by the release of these new findings.

The bed-load transport rate in transverse (y) direction on transverse sloping beds is modelled by:

$$q_{bed\,y} = -q_{bed\,x} G \frac{dz_b}{dy} \qquad (1)$$

with: G = transverse bed slope coefficient, q_{bedx} = bed-load transport rate in longitudinal (x) direction, per unit width and q_{bedy} = bed-load transport rate in transverse (y) direction, per unit width, z_b = bed surface level.

Longitudinal and transverse bed-load transports are governed by a mechanical balance of forces of particles traveling over the sloping bed surface. The transverse bed slope coefficient (G) is a function of flow conditions and grain size. In general the G-value may range between 2 á 3 (theoretical maximum: from angle of repose: Engelund 1976) to 0.2 á 0.3 (smallest value, measured by Hasegawa 1981). The general accepted functional dependency is:

$$G \sim 1/\sqrt{\theta} \qquad (2)$$

with: θ = Shields parameter.

In bed leveling experiments the transverse slope parameter is determined from measured transverse transport (bed leveling rate) and measured longitudinal bed-load transport. In flume tests it is easier to measure the total transport rate than to measure the bed-load transport rate. If no distinction is made between bed-load transport and suspended-load transport the formula for transverse slope effects reads:

$$q_{bed\,y} = -q_{totalx} G_{total} \frac{dz_b}{dy} \qquad (3)$$

with: G_{total}= transverse bed slope coefficient to total load, q_{totalx} = total transport rate.

Though, from a mechanical point of view, suspended load is not involved in the transverse slope process, Eq.(3) is useful to compare results of different tests.

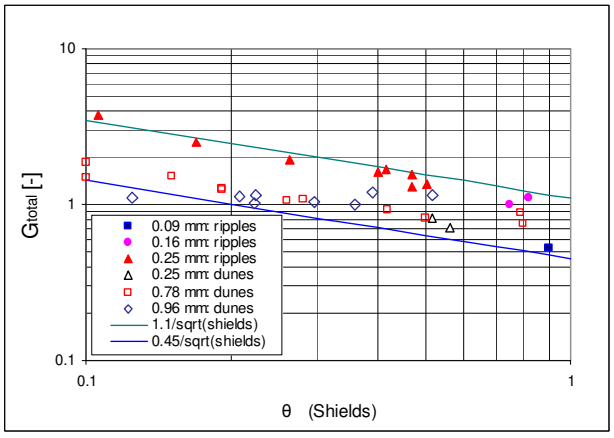

Figure I-3: Transverse slope parameter, related to total transport, for fine to coarse sands in Delft and Darmstadt bed levelling experiments as a function of Shields parameter.

Results of bed-leveling experiments in Darmstadt and Delft, with G calculated on basis of total load transport (Eq. 3) are compiled in Fig. I-3. These experiments are described in Talmon et al. 1995, Wiesemann et al. 2004 and Wiesemann et al. 2006ab.

Figure I-3 shows that the transverse slope parameter, based on total load, is found between two lines: $0.45/\sqrt{\theta} < G_{total} < 1.1/\sqrt{\theta}$. Fine sands of 160 and 250 µm behave different than 780 µm sand. These fine sands are found along the upper boundary. Their bed was rippled, and suspended-load occurred. For θ<0.5 their transverse slope effect is a factor two stronger than that of coarse 780 µm sand, which did not involve suspended-load transport. Amongst the fine sands of 160 & 250 µm and the finest sand of 90 µm the transverse slope effect is distinctly different (a factor of two). The transverse slope parameter of the very recently released Darmstadt 960 µm data is similar to that of 780 µm Delft data for 0.2< θ<0.4. Delft data is referenced by median grain size: d_{50}=90, 160 and 780 µm. Darmstadt data is referenced by mean grain size: d_m= 250 and 960 µm. Median grain sizes of the Darmstadt tests are d_{50}=230 and 830 µm.

The formula being employed in calculations for natural rivers is (see Talmon et al. 1995):

$$G = \frac{1}{9}\left(\frac{h}{d}\right)^{0.3} \frac{1}{\sqrt{\theta}} \qquad (4)$$

with: d = particle diameter, h = water depth, $\theta \equiv \frac{\tau}{(s-1)\rho g d}$ = Shields parameter, τ = total bed shear stress, g = gravity, s = relative density (sand 2.65), ρ = fluid density.

This is a formula based on integral parameters (water depth h and Shields parameter including form drag of bed features).

In the present contribution it is focused on processes at the surface of the bed. The formulae being employed are known from earlier studies on bed-load transport and bed slope effects (Ashida and Michiue 1972, Engelund and Fredsoe 1982, Hasegawa 1981). Numerical values of parameters are re-evaluated by considering regime influences, measured longitudinal transport and measured transverse transport.

II. DATA

Typical conditions in the Delft bed levelling experiments are summarised in Table II-1. Bed-load transport was measured by gathering sand at the end of the flume and suspended-load transport was subtracted, if present. The transverse slope parameter (G) was determined by the levelling rate of initially prepared transverse beds. The driving force of bed-load transport is difficult to measure. A measurable property of bed-load transport is the transport rate. The measured transverse slope parameter is shown in Figure II-1 as a function of the dimensionless transport rate of bed-load:

$$q_b^* = \frac{q_{bed\ x}}{\sqrt{(s-1)gd^3}} \qquad (5)$$

Experiments labelled T1-T11 are coarse grain, bed-load only, conditions (dunes). The experiments labelled run2, run4 and run5 are experiments involving suspended-load transport and rippled beds.

Suspension concentrations were measured by iso-kinetic sampling. Suspended load was about 50% of total transport. Examples of suspended load profiles are shown in Figure II-2. The scatter in the data points is attributed to distortion of the flow by the presence of ripples. The flow was rather shallow. The ripples typically extended about 1 cm above mean bed level.

Table II-1: Characteristic conditions Delft bed levelling experiments

Experiment	d_{50} [µm]	h [m]	U [m/s]	θ [-]
T1-T11	780	0.14-0.44	0.39-0.75	0.1-0.8
run 2	90	0.07	0.22	0.90
run 4	160	0.07	0.28	0.82
run 5	160	0.033	0.22	0.75

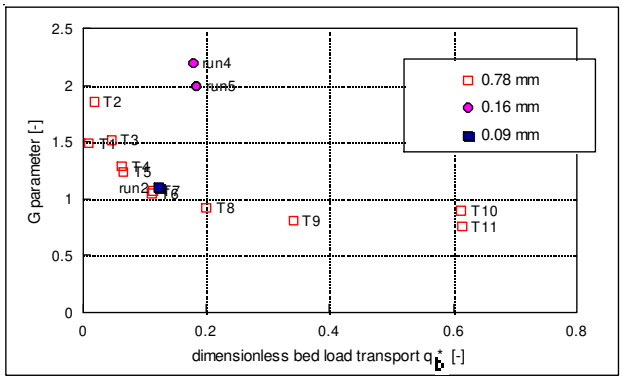

Figure II-1: Dimensionless bed-load transport and transverse slope parameter in Delft bed levelling experiments.

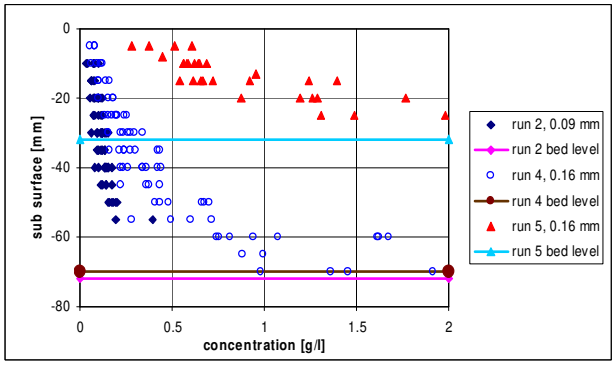

Figure II-2: Concentration profiles measured in Delft suspended load tests.

The conditions in the Darmstadt bed levelling experiments are summarized in Table II-2. The 250 µm tests had ripple covered beds, except for the two highest transport rates where dunes occurred. All 960 µm tests had dune covered beds. In both series the longitudinal transport rate was measured by gathering the sand at the end of the flume too, but there were no measurements conducted which lead to information about the suspended-load concentrations. Additionally to the measurements of a sand trap set-up the longitudinal transport rates were evaluated by considering the movement of the bed forms/dunes in the measuring section. This led to more reliable results regarding to the correlation of Shields parameter to the transport rate. To make these results comparable to the series with the fine sand a small factor was used to shift the bed-load results in the region of the measurements conducted by using the sand trap at the end of the flume. So the total amount of longitudinal transport was measured with a comparable method to the fine sand experiments but the correlation of the transport rates of the dune-experiments was increased by using the bed form-travelling method (Wiesemann et al. 2006b).

The measured transverse slope parameter (to total transport) is shown in Figure II-3 as a function of the dimensionless total transport rate. For coarse material this equals the dimensionless bed-load transport rate.

Figure II-1 shows that fine sand (90 µm) and coarse sand (780 µm) lie within a lower band of G-values. Material in between, 160 µm, shows a stronger bed slope effect.

Figure II-3 shows that at the lowest transport rates, the transverse slope parameter of 960 µm sand is somewhat lower than for 250 µm sand if evaluated on basis of total transport. If 250 µm sand would have been evaluated on basis of longitudinal bed-load transport (for which no data is available), a similar trend to that shown in Figure II-1 would result, giving distinctly higher G-values for 160 and 250 µm sands.

Table II-2: Characteristic conditions Darmstadt bed levelling experiments

experiment	d_m [µm]	h [m]	U [m/s]	θ [-]
Series R0	250	0.30	0.22-0.64	0.11-0.57
Series R1	960	0.30	0.48-0.77	0.12-0.53

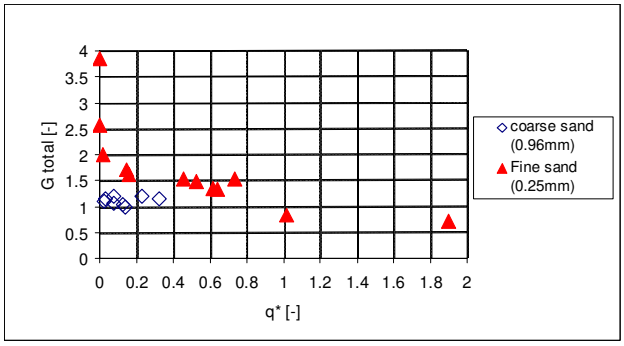

Figure II-3: Dimensionless total transport and transverse slope parameter (to total transport) in Darmstadt bed levelling experiments.

The results of all bed levelling experiments (G parameter) are compared to the empirical field equation for natural rivers (Eq. 4) in Figure II-4 and Figure II-5. It is to be mentioned that the equation for natural rivers was derived from field experience in combination with results of the 780 µm data-set. Figure II-4 shows major differences between the suspended-load experiments (run4, 5 versus run2) and a major deviation of the experiments run4 and run5 from Eq. (4).

Figure II-5 shows that the Darmstadt coarse sand data, corresponds reasonable to the formula for natural rivers

Eq. (4). If the 250 μm experiments would be corrected for suspended-load transport, these points would shift upward, and the same tendency would emerge as for run 4 and run 5 shown in Figure II-4.

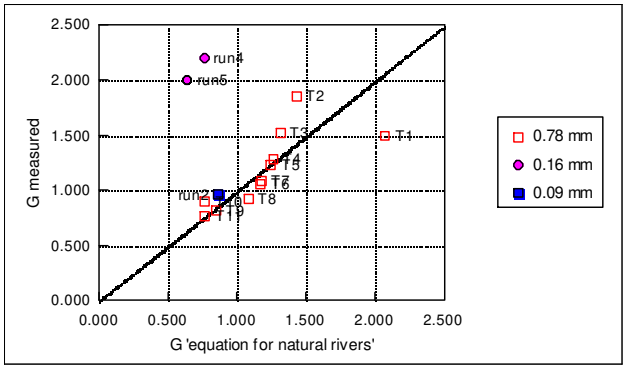

Figure II-4: Comparison of the transverse bed slope parameter for natural rivers (Eq. 4) with the results of Delft straight flume bed levelling experiments.

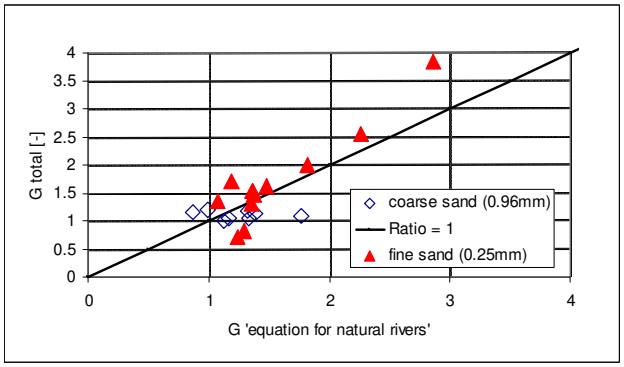

Figure II-5: Comparison of the transverse bed slope parameter for natural rivers (Eq. 4) with the results of Darmstadt straight flume bed levelling experiments (to total load).

III. FLAT BED THEORY: MATHEMATICAL MODELLING OF TRANSVERSE SLOPE EFFECTS

Bed-load transport follows from a mechanical balance of travelling bed-load particles. The employed formulas for longitudinal transport and transverse slope effect do not differ much from the mechanical approach followed by Engelund and Hansen 1967 and Ashida and Mitchieu 1972 (a description is given in Kovacs and Parker 1994). Assumptions are: 1) Mechanical processes at the bed surface determine the bed slope effect (equilibrium of forces and continuity). 2) Suspended load transport is not influenced by bed slope. 3) Time-average modelling of transport processes suffices to capture governing physics (no need for dynamic simulation of saltations). 4) Lift forces are negligible. 5) The influence of density driven flow along transverse slopes is negligible. Concentration measurements given in Talmon 1991 show that the transverse variation of concentration is small. The dimensionless transport rate of bed-load is:

$$q_b^* \equiv \frac{q_{bed\,x}}{\sqrt{(s-1)gd^3}} = \frac{\sqrt{a}}{\mu_c}\left(\theta' - \theta_{cr}\right)\left(\sqrt{\theta'} - \sqrt{\theta_0}\right) \qquad (6)$$

with: $u^* \equiv \sqrt{\tau'/\rho}$ = friction velocity to the grains, μ_c= dynamic granular friction coefficient, τ' = shear stress on the grains, θ_{cr} = critical Shields parameter (at incipient erosion),

$$\theta' \equiv \frac{\tau'}{(s-1)\rho g d} = \text{Shields parameter to the grains,} \qquad (7)$$

$$\theta_0 \equiv \frac{4}{3}\frac{\mu_c}{aC_d} = \text{dynamic granular friction / fluid drag,} \qquad (8)$$

with: C_d = drag coefficient particles

$$\sqrt{a} \equiv \frac{U}{u_*} = \text{fluid velocity ratio} \qquad (9)$$

with: U = fluid velocity at particle height

Transverse bed-load transport on a sloping bed follows from a two-dimensional force balance of bed-load transport. The coefficient in the transverse slope formula is:

$$G = \frac{1}{\mu_c}\sqrt{\frac{\theta_0}{\theta'}} \qquad (10)$$

The same variables emerge in the formulae for both q_b^* and G, because the formulae stem from one force balance. The variables in these equations are: flow velocity at particle height, friction velocity, drag coefficient and dynamic friction coefficient. Appropriate values pertaining to governing flow regimes have to be established. Regimes are determined by particle Reynolds number and consideration of the average vertical position of travelling bed-load in the turbulent boundary layer.

The particle diameter is an important factor:

- In case of coarse sands bed-load travels in the buffer region of the velocity profile. The flow above the sand bed is hydraulically rough. In hydraulically rough flow the travelling height of the particles scales with the particle diameter (Ashida & Michieu 1972). In case of fine sand, the flow is hydraulically smooth and bed-load travels at the edge of the laminar sublayer. At this level the flow velocity is less.
- The drag coefficient of particles is influenced by particle diameter. The microscopic flow around coarse particles is turbulent. The flow around fines is laminar, consequently higher drag coefficients apply and vary with the particle-Reynolds number.

The average velocity difference (*U-V*= slip velocity) between the fluid and the particle is important to particle drag regime. This velocity difference follows from a balance of forces (hydrodynamic drag, submerged weight of particles, bed-grain friction):

$$U - V = U\sqrt{\frac{4}{3}\frac{\mu_c}{aC_d\theta'}} = U\sqrt{\frac{\theta_0}{\theta'}} \qquad (11)$$

with: V = particle velocity parallel with the bed.

Viscosity influences the drag of small particles. The Reynolds number of fluid drag of these particles is:

$$Re = \frac{(U - V)d}{\nu} = \sqrt{\frac{4}{3}\frac{\mu_c}{C_d}d^{*3}} \qquad (12)$$

with:

$$d^* = d\left(\frac{(s-1)g}{\nu^2}\right)^{1/3} \qquad (13)$$

Particle and fluid properties are accommodated in the dimensionless particle diameter d^*. Fluid and flow properties are accommodated in the drag coefficient C_d. At $Re < 1$, the Stokes regime, the drag coefficient is given by $C_d = 24/Re$. At high Reynolds number the C_d is constant: for a smooth sphere, at high Reynolds: $C_d = 0.4$, for irregular spheres at high Re: $C_d = 1.25$, Chien (1994). The transitional and Stokes regimes, which are applicable to our conditions, might be described by one formula (Shiller & Naumann 1933):

$$C_d = \frac{24}{Re}(1 + 0.15\,Re^{0.687}) \text{ , valid for } Re<800 \qquad (14)$$

Examples of numerical values are: C_d = 24 at Re = 1 (laminar regime), C_d = 4.15 at Re = 10 (transitional regime), C_d = 1.09 at Re = 100 (transitional regime). Combining Eq. (12) and Eq. (14) leads to the conclusion that the 90 μm and 160 μm sands of the Delft experiments are within Stokes range. Reynolds numbers are respectively Re ~0.15, and Re ~1. The 780 μm sand is within the turbulent drag regime.

Another parameter is the fluid velocity (U) at average particle transport height. The average transport height of particles was assumed proportional to particle diameter:

$$z = nd \text{ , } (n= 2, \text{ Ashida Michieu}) \qquad (15)$$

Particle diameters are non-dimensionalised the same way as the profile coordinate of turbulent boundary layer flow:

$$d^+ = \frac{u^* d}{\nu} \quad , \quad z^+ = \frac{u^* z}{\nu} \qquad (16)$$

At a transport level of n=1 á 2 the 90 μm sand will be transported in the laminar sublayer (z^+<11) region; because d^+= 1.2 at θ'= 0.15 which is a typical value. The 160 μm sand will also be transported in the laminar sublayer region: d^+= 3.2 at θ'= 0.15. The 780 μm sand is transported in the logarithmic fully turbulent (z^+>70) region: d^+=39 á 137 , at 0.05<θ' <0.15.

At 960 μm the sand will be transported in the fully turbulent region, because all the different runs have values of d^+ which are larger than 70. The 250 μm sand lead to values which are in the transitional buffer region. Only two experiments in the R0 series, in which dunes were present, might lead to larger values in the fully turbulent region.

In Section IV the appropriate numerical values for C_d and $a = (U / u^*)^2$ will be identified by consideration of the above theory and available data.

IV. Transverse Bed Slope Effect in Ripple and Dune Regime

To calibrate the parameters-values in the transverse slope theory, it is noticed that longitudinal and transverse transports are governed by the same fundamental physical processes. This means that sediment transport in both transport directions is governed by one and the same bed-load transport model. It must be possible to obtain fair agreement between available data on both transports and mathematical formulation.

For longitudinal bed-load transport a generalized form of Eq. (6) is used, with a multiplication factor A to accommodate typical conditions in ripple and dune regime:

$$q_b^* = \frac{q_{bed\,x}}{\sqrt{(s-1)gd^3}} = A\frac{\sqrt{a}}{\mu_c}\left(\theta_{eff} - \theta_{cr}\right)\left(\sqrt{\theta_{eff}} - \sqrt{\theta_0}\right) \qquad (17)$$

in which: A = constant to accommodate bed form properties. θ_{eff} = effective Shields number to the grains. The formula for the transverse slope coefficient is generalized to:

$$G = B\,\frac{1}{\mu_c}\sqrt{\frac{\theta_0}{\theta_{eff}}} \qquad (18)$$

with: B = constant to accommodate bed form properties.

Bed-load transport processes are governed by fluid mechanical stresses acting on the grains. In case of dunes, the bed shear stress at the top of the dune is calculated by assuming a fully developed turbulent flow above the dune top. The bed shear stress distribution over the face of the dune is calculated on the assumption of similarity of dune-shape profiles, Talmon 1997. Bed-load transport in longitudinal and transverse direction is

calculated by integration of shear stress over one dune. The grain shear stress at the top of the dune is substituted for the effective Shields number in Eq. (17) and (18): $\theta_{eff} = \theta'_{top}$ Integration of bed-load transport in longitudinal and transverse direction over dune profile gives theoretical values of A=2/3 and B=1.05. The grain shear stress at the top of the dune is then calculated from $k_s=3*d_{90}$, local water depth above the dune and flow velocity above the dune. In the analysis of the 780 µm T1-T11 experiments, measured dune height were used to determine θ'_{top}. For field conditions the dune height predictor by van Rijn might be applied.

In the ripple regime such a type of integration method is not applicable because the flow is different and saltation lengths are greater. The shear stress at the grains is calculated from $\theta_{eff} = \theta' = 0.2\,\theta$ for the 90 and 160 µm experiments. This relation was established by evaluation of realistic parameter values for the variables in Eq. (17) and Eq. (18). The overall Shields value was calculated from the measured hydraulic energy gradient. A quasi flat bed is assumed by default: A=1 and B=1.

Of these Delft experiments, first the coarse grain 780 µm experiments were analyzed. At $\sqrt{a} = 6.8$ [1] and C_d = 0.8 a fair agreement of longitudinal transport and transverse slope parameter is obtained, see Figure IV-1, is employed. For the fine sands investigated, a suitable ratio of the local flow velocity and friction velocity u_* is $\sqrt{a} = 2.5$. For 90 and 160 µm sand values of C_d = 6 respectively C_d =15 apply well. In the average C_d value of bed-load, account was made for the dynamical character of bed-load transport. The velocity difference with the fluid is larger than the theoretical value, because of saltation of the grains. Consequently in the laminar drag regime, on the average, smaller C_d values have to be employed than theoretically because the actual Re particle number is larger. For coarse grains C_d =0.8 value is appropriate (non-spherical particle in turbulent drag regime). An overview of employed parameter values in calculations is given in Table IV-1.

The Darmstadt 250 data can not be analysed similarly because the suspended-load transport was not measured. So there is no information on longitudinal bed-load transport.

In the 960 µm experiments dunes were present. The relevant Shields parameter is nevertheless calculated from roughness height $k_s=3*d_{90}$ and mean flow depth. This series leads to A=0.72 and B=1.06. The results are shown in Figure IV-2. The parameters are comparable to those in the 780 µm T1-T11 experiments, even though this time mean flow depth and mean flow velocity were used.

[1] this is smaller than Kovacs and Parker 1994 who use $\sqrt{a} = 11$.

Table IV-1: Overview of parameter values in analysis of transverse bed slope influence.

model parameters	90 µm	160 µm	780 µm	960 µm
d^*	2.13	4.05	19.9	24.1
θ_{eff}	0.17	0.15	0.02-0.14	0.04-0.10
d^+	1.5	3.2	12.6 - 90	69.5-111
μ_c	0.3	0.3	0.4	0.3
$\sqrt{a}$	2.5 (z^+=2.5)	2.5 (z^+=2.5)	6.8 ($z=k_s/2$)	7.8
C_d	6	1.5	0.8	0.8
Re	0.8	4.2	72	83.8
θ_0	0.0107	0.042	0.014	0.01
θ_{cr}	0.12	0.066	0.029	0.03

Measured and calculated longitudinal bed load transport of Delft tests is shown in Figure IV-3 (including all suspended load experiments of Talmon 1992 in 180° bend flume).

Measured and calculated transverse slope parameter of Delft tests are shown in Figure IV-4. This graph shows that fair agreement between theory and measurement is achieved when regime influences for fine and coarse sand are accounted for.

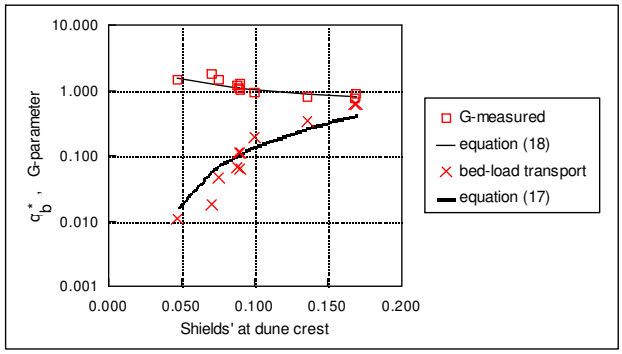

Figure IV-1: Bed-load transport and transverse slope parameter in dune-regime: 780 µm sand data and calculations by Eq.(17) and Eq.(18).

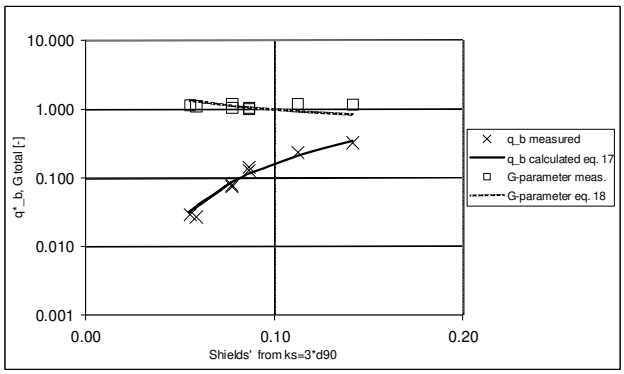

Figure IV-2: Bed-load transport and transverse slope parameter in dune-regime for 780 µm series R1: laboratory data of Wiesemann and calculations by Eq.(17) and Eq.(18).

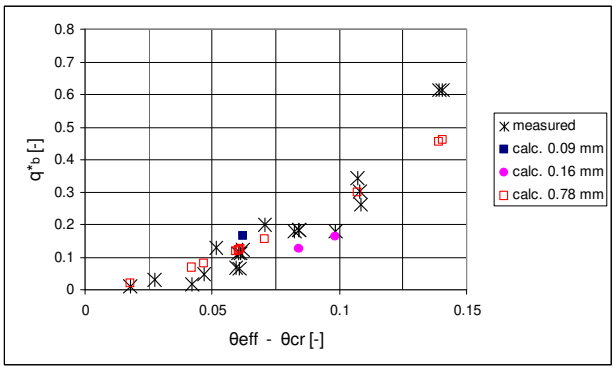

Figure IV-3: Measured and calculated dimensionless longitudinal bed load transport of 90, 160 and 780 µm sands as a function of the dimensionless shear stress at grains minus critical shear stress (ripples: $\theta_{eff}=0.2\ \theta$, dunes: $\theta_{eff}=\theta'_{top}$).(97Tmod05.xlw)

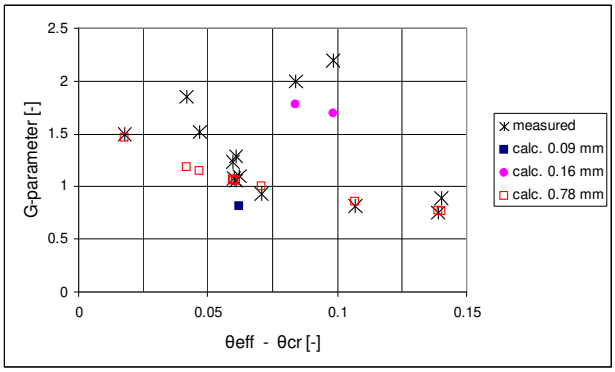

Figure IV-4: Measured and calculated transverse bed slope parameter of 90, 160 and 780 µm sand as a function of the dimensionless shear stress at grains minus critical shear stress (ripples: $\theta_{eff}=0.2\ \theta$, dunes: $\theta_{eff}=\theta'_{top}$). (97Tmod05.xlw)

V. CONCLUSIONS

The measured values for the transverse slope coefficient related to bed-load, for 90-960 µm sand, are within a range of $0.7<G<4$.

By using the force balance of bed-load particles, an unification of longitudinal and transverse bed-load transport has been achieved for the fine grain ripples regime and the coarse grain dune regime. This way numerical values for the transverse slope parameter (G) are found for different conditions. It is concluded that account has to be made for flow conditions at the traveling height of the particles and particle drag conditions.

Grain shear stresses have to be predicted beforehand. In the dune regime dune height has to be predicted also (which might explain the role of d_{50}/h in the equation for natural rivers). The model should be tested further against recent field experience.

Further laboratory tests are advised, because more data on the transverse bed slope influence, under conditions of fully developed bed forms, is needed urgently. Specifically in the regime of 100 to 600 µm sand more data is needed. In such experiments, suspended load transport has to be measured also. This has to be deducted from measured total transport for determination of bed-load transport. Such strategic data will serve to improve confidence in the outcome of numerical models.

ACKNOWLEDGMENT

Thanks to Dr Erik Mosselman, Dr Kees Sloff and Dr Peter Mewis for bringing parties together within a framework of coordination of river-bound transverse bed slope activities. Thanks to Dirk Jan Walstra and Kees Kuijper for sharing experience on estuary and sea research. Thanks to Prof. Dr Leo van Rijn for inspiring discussions on transverse slope effects. This work was partly funded the by the National Institute for Coastal and Marine Management (RIKZ) of the Dutch Ministry of Transport, Public Works and Water Management.

NOTATIONS

a	square of velocity ratio $a=(U/u^*)^2$
A	constant to accommodate bed form properties
B	constant to accommodate bed form properties
C_d	drag coefficient particles
d	particle diameter
d_{50}	median sand diameter
d^*	dimensionless particle diameter
d^+	particle diameter in boundary layer coordinates
g	gravitational acceleration
G	transverse bed slope coefficient
G_{total}	transverse bed slope coefficient to total load
h	local water depth
k_s	equivalent (Nikuradse) sand-roughness
n	porosity
n	constant in travelling height particle
q	sediment transport rate per unit width (volume, incl. pores)
$q_{bed\ x}$	bed-load transport in x-direct. (incl. pores)
$q_{bed\ y}$	bed-load transport in y-direct. (incl. pores)
q^*	dimensionless total transport rate
$q_b{}^*$	dimensionless transport rate bed-load
q_{total}	total transport rate
Re	Reynolds number particle
s	relative density
U	fluid velocity at mean particle height
u^*	friction velocity
V	particle velocity parallel to the bed
x	coordinate in streamwise direction
y	coordinate transverse direction
z_b	bed surface level
z^+	coordinate boundary layer flow
μ_c	dynamic granular friction coefficient
ν	kinematic viscosity
θ	Shields parameter
θ'	Shields parameter to the grains
θ_{cr}	critical Shields parameter
θ_{eff}	effective Shields parameter to the grains

θ_0	parameter in transport model (ratio of Coulomb friction and fluid drag)
ρ	density water
ρ_s	density sediment
τ	total shear stress
τ'	grain shear stress
ψ	direction bed load transport

REFERENCES

[1] Ashida K. & Michiue M, 1972, Study on hydraulic resistance and bedload transport rate in alluvial streams, *Trans. Japan Soc. Civ. Engrg.*, Vol 206, pp.59-69.

[2] Bendegom, L. van, 1947, Eenige beschouwingen over riviermorphologie en rivierverbetering, De Ingenieur, Vol.59, No.4, pp.B1-B11, in Dutch, English translation: Some considerations on river morphology and river improvement, Nat. Res. Council of Canada, Tech. Transl. 1054, 1963.

[3] Chien, S.F., 1994, Settling velocity of irregularly shaped particles, SPE Drilling and Completion, paper 26121

[4] Engelund, F., 1976, Experiments in curved alluvial channel, part 2, Progress Rep.38, Tech. Univ. Denmark, pp.13-13.

[5] Engelund, F. and E. Hansen, 1967, A monograph on sediment transport in alluvial streams, Teknisk Forlag, Copenhagen, Denmark, pp.62.

[6] Engelund, F. and J. Fredsºe, 1982, Hydraulic theory of alluvial rivers, Advances in Hydroscience, Vol.13, pp.187-215.

[7] Hasegawa, 1981, Bank-erosion discharge based on a non-equilibrium theory, Trans. JSCE, Vol.13, pp202-205 (in Japanese).

[8] Kovacs, A. & G. Parker, 1994, A new vectoral bed load formulation and its application to the time evolution of straight river channels, J. Fluid Mech., Vol.267, pp.153-183.

[9] Shiller J. and A Naumann, 1933, Uber die grundlegende berechnungen bei der schwerkrachtaufbereitung, Ver. Deunt. Ing. vol 77, p318.

[10] Struiksma N., Olesen, K.W., Flokstra, C. and H.J. de Vriend, 1985, Bed deformation in alluvial channel bends, J. Hydr. Res., IAHR, Vol.23, No.1, pp.57-79.

[11] Talmon, A.M., 1991, Suspended sediment transport in axi-symmetric river bends , in Soulsby & Bettess (eds), Sand Transport in rivers estuaries and the sea, proc. Euromech 262, Wallingford, England, Balkema publ.

[12] Talmon, A.M., 1992, Bed topography of river bends with suspended sediment transport, Doctoral thesis, Delft Univ. of Technol., (also: Communications on Hydr. and Geotechnical Engrg., Delft Univ. of Technol., Dept. of Civil Engrg., Rep.92-5, ISSN 0169-6548).

[13] Talmon, A.M., 1997, Sediment transport in dune regime and transverse slope effect (in Dutch, sediment transport bij duinen en invloed dwarshelling), Delft Hydraulics, J1234.

[14] Talmon, A.M., M.C.L.M. van Mierlo & N. Struiksma, 1995, Laboratory measurements of the direction of sediment transport on transverse alluvial-bed slopes, J. Hydraulic. Res., vol.33, no 4, pp.495-517.

[15] Wiesemann, J.-U., Mewis, P., Zanke, U., 2004, Laboratory measurements of sediment transport on transverse sloped beds, Singapore, Second International Conference on Scour and Erosion, Proceedings, Volume 2, pp. 252-259.

[16] Wiesemann, J.-U., Mewis, P., Zanke, U, 2006a, Bed Levelling Investigations on Transverse Sloped Beds, **submitted** for the International Conference of River Hydraulics - Riverflow 2006, Lisboa, Portugal.

[17] Wiesemann, J.-U., Mewis, P., Zanke, U, 2006b, Sediment Transport Rate in the Dune Regime in Bed Levelling Experiments, **submitted** to the International Conference on Scour and Erosion ICSE3 2006, Netherlands.